Ammonia Absorption at Haber Process Conditions

Mark S. Huberty, Andrew L. Wagner, Alon McCormick, and Edward Cussler
Dept. of Chemical Engineering and Materials Science, University of Minnesota, Minneapolis, MN, 55455

DOI 10.1002/aic.13744

The kinetics of ammonia absorption into magnesium chloride is measured as ammonia pressure change in the temperature range 170-430°C. The actual pressure minus that at equilibrium drops quickly, with a half life of less than a minute. It varies with the square-root of time, suggesting diffusion limited absorption. The diffusion coefficient of ammonia in solid magnesium chloride inferred from these data is on the order 10^{-11}-10^{13} cm^2/s, considerably faster than many solid-phase diffusivities. While optical microscopy and BET surface area experiments indicate recrystallization and agglomeration of the absorbent at ammonia synthesis temperatures, the absorption rate remains high. The dependence of absorption rate on temperature, particle size and the presence of a silica support is also investigated. The results suggest both improved ammonia separation and ways to develop high-conversion, small-scale, multifunctional ammonia synthesis reactors.
© 2012 American Institute of Chemical Engineers *AIChE J,* 58: 3526–3532, 2012
Keywords: absorption, diffusion

Introduction

For the last century, the chemical industry has depended on feedstocks of fossil fuels. These feedstocks can be delivered centrally, from a pipeline, a tanker, or a train of coal cars. The chemical industry that has evolved under these conditions is highly centralized around large, carefully optimized plants. It has effectively produced large quantities of inexpensive fuels, textile fibers, and fertilizers, which have supported the development of modern civilization.

Now, the limits on fossil fuel reserves may change this structure. The manufacture of small amounts of highly specialized chemicals, like pharmaceuticals, will still occur in a few specialized plants. However, the manufacture of some fuels and fertilizers may take place in small dispersed plants. One good example is liquid fuels made from biomass. These are less likely to be made in large complex plants because collecting the biomass will take too much energy. Such biomass-based fuels are more likely to be made in small simple plants making products for a local market. Thus, a new commodity chemical industry may depend on distributed, not centralized, manufacture.

Ammonia, the key fertilizer responsible for the green revolution, is one compound which may be made in this distributed fashion. Ammonia is made from nitrogen and hydrogen. Nitrogen can be separated from air at large scale by cryogenic distillation and at small scale using selective hollow fiber membranes. Hydrogen can be made at large scale from the incomplete combustion of natural gas, or at small scale from the electrolysis of water. The nitrogen and hydrogen are then combined at 120 bar and 380°C to make ammonia. These high pressures and temperatures are needed to achieve fast reactions, typically taking less than a minute. However, single-pass conversion is modest, around 20%,[1] so the process requires separating the ammonia, and recycling the unreacted nitrogen and hydrogen. This separation and recycle adds complexity to the process. Such complexity can make distributed manufacture of ammonia less likely.

In this article, we seek a solid absorbent for ammonia which can enhance the effective conversion and simplify ammonia synthesis. The absorbent should be able to operate at the current reaction temperature and pressure. It should operate over many cycles of loading and unloading. Most importantly, the absorption and desorption should be fast, about as fast as the reaction itself.

In this article, we test magnesium chloride as a possible absorbent for ammonia. Studies in the literature show that this compound can absorb much more ammonia than other, more conventional materials, as shown in Table 1.[2–7] The absorbent takes up ammonia in three distinct complex formation steps

$$\begin{aligned}
&\mathrm{MgCl_{2(s)} + NH_{3(g)} \rightleftharpoons Mg(NH_3)Cl_{2(s)}}\\
&\mathrm{Mg(NH_3)Cl_{2(s)} + NH_{3(g)} \rightleftharpoons Mg(NH_3)_2Cl_{2(s)}}\\
&\mathrm{Mg(NH_3)_2Cl_{2(s)} + 4NH_{3(g)} \rightleftharpoons Mg(NH_3)_6Cl_{2(s)}}
\end{aligned}$$

Absorption at lower temperatures uses all three reactions as a means of storing energy for automobiles: the ammonia is released from the magnesium chloride by warming and catalytically decomposed into hydrogen, which is then burned in an engine.[8] Absorption at the high ammonia synthesis reactor temperatures uses only the first reaction. However, the mechanism and the kinetics of this absorption at these temperatures are not known, and are explored in this article.

Theory

We will measure the kinetics of ammonia uptake as changes in ammonia pressure in a small cell of fixed volume

---

Correspondence concerning this article should be addressed to E. Cussler at cussl001@umn.edu.

Table 1. Equilibrium Ammonia Uptake by Magnesium Chloride and by Other Absorbents and Adsorbents

	Absorption Capacity at 40 kPa and 25°C (mmol NH_3/g)	Equilibrium Pressure of First Ammonia at 430°C (bar)	Gravimetric Density of Complex (g NH_3/g complex)	Volumetric Density of Complex (g NH_3/cm^3 complex
$MgCl_2$	$54.8^{(4)}$	$3.9^{(8)}$	$0.52^{(2)}$	$0.62^{(2)}$
$CaCl_2$	$0.2^{(4)}$	$125.8^{(8)}$	$0.58^{(2)}$	$0.68^{(2)}$
$MgCl_2$–$CaCl_2$	$36.8^{(5)}$	–	–	–
AC	$1.19^{(6)}$	$3.6 \times 10^{-5(7)}$	–	–
HNO_3–AC	$3.07^{(6)}$	–	–	–
Na–Y zeolite	$6.14^{(6)}$	–	–	–
Cu–Y zeolite	$9.34^{(6)}$	–	–	–
Mordenite	–	$1.2 \times 10^{-8(3)}$	–	–

Experiments reported in Ref. 6 were conducted at 50°C. HNO_3-AC refers to activated carbon doped with nitric acid. Superscripts refer to the reference providing the value.

held at constant temperature. When the cell contains no magnesium chloride, its pressure is constant for more than 6 h. When the cell does contain the chloride, its pressure drops over minutes. In this case, the uptake of ammonia is described by

$$\frac{V}{RT}\frac{dp}{dt} = -AK(p - p*) \tag{1}$$

where V is the cell volume, R is the gas constant, T is the temperature, p is the pressure, A is the surface area of the absorbent, and t is the time. The pressure p^* is the value of the pressure at equilibrium, when no further uptake occurs.

The rate constant K is the quantity which we want to measure. If the ammonia uptake is by adsorption on the surface, then K includes the mass transfer in the gas k_p and the surface reaction k_s

$$\frac{1}{K} = \frac{1}{k_p} + \frac{1}{k_s} \tag{2}$$

Note that k_p can vary with stirring in the gas, and that k_s is often a strong function of temperature. All these k's have dimensions of mole per area per pressure per time. Because K is not a function of time, the integration of Eqs. 1 and 2 gives

$$\ln\left[\frac{p - p*}{p_0 - p*}\right] = -K\left(\frac{ART}{V}\right)t \tag{3}$$

If the function of pressure on the left is plotted vs. time, the slope can be used to find K.

Conversely, if the ammonia uptake is by absorption into the solid, then

$$K = \left(\sqrt{\frac{D}{\pi t}}\right)H \tag{4}$$

where D is the diffusion coefficient of ammonia in the solid, and H is a partition coefficient, the ratio of the ammonia concentration in the solid, in moles per volume, to the ammonia pressure.[9] Integrating Eqs. 1 and 4 gives

$$\ln\left[\frac{p - p^*}{p_0 - p^*}\right] = -\left(\frac{ART}{V}\right)\sqrt{\frac{4D}{\pi}}H\sqrt{t} \tag{5}$$

The variation of pressure on the left hand side of Eq. 5 is the same as that on the left hand side of Eq. 3 but the variation with time on the right hand side is different. The variation with the square root of time is the signature of a diffusion-controlled process.

Those skilled in the study of mass transfer will correctly point out that Eq. 5 is a major approximation in two ways. First, it assumes no resistance in the gas phase: that is, it assumes that the analog of k_p in Eq. 2 is large. Second, it assumes that our experiments are limited to small times. We will show in our experiments that each of these approximations is reasonable. We turn now to these experiments. It bears noting that the above analysis is valid only for isothermal conditions, and therefore, the temperature must be held relatively constant during the experiments.

Experimental

Materials

The absorbent, >98% anhydrous magnesium chloride (Sigma-Aldrich, St. Louis), was ground using mortar and pestle and sieved to various apparent particle sizes. The magnesium chloride samples used in much of this work, on order of 200 μm, were passed by a 425-μm sieve but retained by a 212-μm sieve. For convenience, the samples were identified by this apparent particle size rather than by the altered particles size that develops during cycles of absorption and desorption at elevated temperature. Anhydrous ammonia gas at 99.99% purity was purchased from Airgas (St. Paul). Argon was obtained at 99.999% purity from Minneapolis Oxygen (Minneapolis). Cab-o-Sil fumed silica was purchased from Sigma-Aldrich (St. Louis). Magnesium chloride was supported on Cab-o-sil using an incipient wetness impregnation technique: 5.0 g of anhydrous magnesium chloride were dissolved in 70 mL of ethanol and stirred for 1 h on a heated stir-plate at 30°C. Then, the solution was added to 3.75 g of Cab-o-Sil and placed in a vacuum oven set at 240°C overnight.

Absorption

The absorption experiments were made in the apparatus shown in Figure 1. The 55-cm^3 stainless steel absorption cell, constructed using Swagelok fittings and 1/2 in. tube, was equipped with a thermowell and a pressure gauge. A Ni–Cr thermocouple from Omega in the thermowell gave the temperature within ±2°C. For most trials, the cell was loaded with 5.0 g of anhydrous magnesium chloride absorbent. Then, the vessel was filled with ammonia or argon and sealed with a valve. Absorption was measured as gas pressure variation with time at temperatures from 25 to 430°C using a Matheson analog mechanical pressure gauge (63-3112) with a range of 0–100 ± 2 psig. Time was measured using a digital stopwatch. Temperature control was not used as the absorption exotherms observed were <5°C due to the

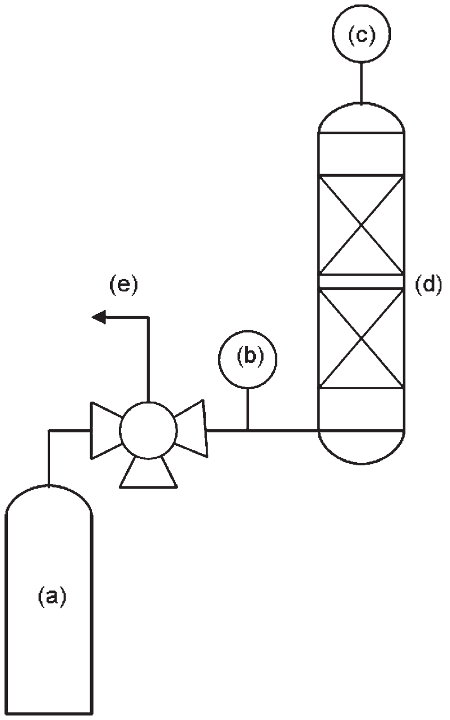

Figure 1. Diagram of the absorption apparatus.

(a) Pressurized ammonia supply, (b) pressure transducer, (c) thermocouple, (d) heated reaction vessel containing 5 g MgCl2, and (e) vent.

relatively small amount of absorbent present. Desorption was achieved by raising the temperature to 450°C and by venting the system to atmosphere for 5 min. Longer venting has no effect on the next absorption cycle. Equilibrium uptake was measured by allowing the cell to equilibrate overnight. Brunauer-Emmett-Teller (BET) isotherms were obtained using a Micromeritics ASAP 200 gas sorptometer and images of the magnesium chloride particles were obtained using a Hirox KH-7700 digital video microscope.

Results

The data are best organized as a test of reproducibility, tests of mechanism and measurements of crystal properties.

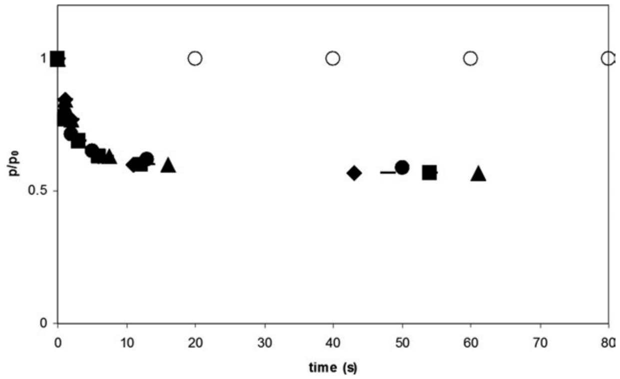

Figure 2. Reproducibility of ammonia absorption experiments at 430°C.

Argon, shown as empty circles, does not show a pressure change. Pure ammonia, shown as filled and dashed points, exhibits reproducible pressure changes. Six consecutive trials on a used absorbent are shown for pure ammonia.

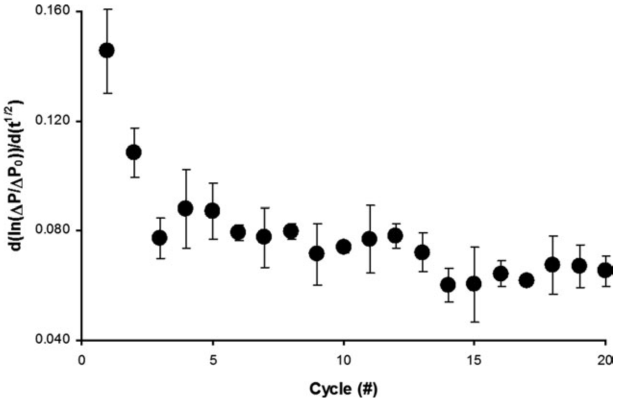

Figure 3. Ammonia absorption rate at 430°C vs. absorption–desorption cycles.

The average slope is of a plot suggested by Eq. 5. The error bars were derived with replicate data.

The reproducibility of these experiments is illustrated by the results given in Figure 2. These runs used 5.0 g of 200 μm magnesium chloride, which had already been used for more than 10 cycles of absorption and desorption. The pressure of argon, shown in Figure 2, is constant over the length of the experiment. The pressure of ammonia dropped quickly over the first few minutes of the experiments. This drop was reproducible with ±15%.

The use of a magnesium chloride sample that has already been used for at least 10 cycles is important, as in shown in Figure 3. The data in that figure show the rate of uptake at 430°C, reported as the change in the logarithm of the system pressure difference per the square root of time vs. the number of cycles to which the chlorine has been subjected. This rate decreases by a factor of two during the first 10 cycles, and then approaches an asymptote. Thus, in our experiments, the absorption becomes somewhat slower when the process is cycled at a constant, high temperature.

Other experiments in the literature have reported data that suggest this is due to a change in microstructure. In particular, studies of room-temperature absorption and higher-temperature desorption argue for an increase in the nanoporosity

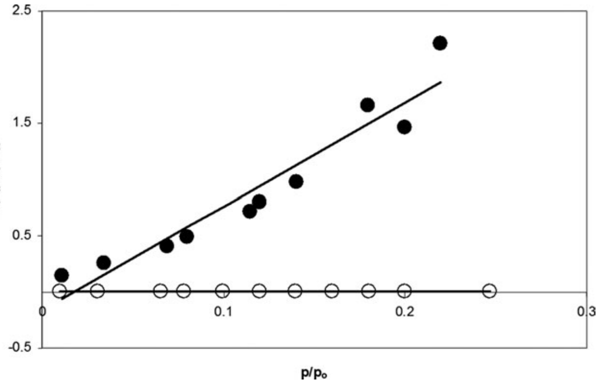

Figure 4. BET isotherms for used anhydrous magnesium chloride (filled circles) and for a silica–alumina reference material (empty circles).

p and p_0 are the equilibrated and saturation pressures of the adsorbate in mmHg and v is the specific adsorbed volume in cm^3/g. The surface area is obtained from the volume of the adsorbed monolayer, which may be determined from the slope and y-intercept.[11]

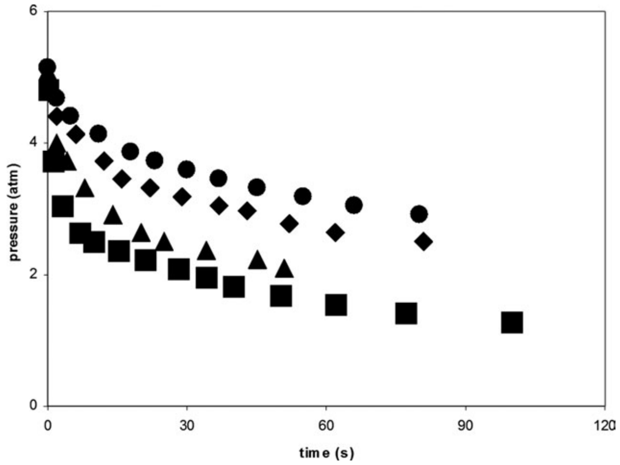

Figure 5. Temperature dependence of ammonia absorption.

The data are for 5 g of unsupported $MgCl_2$ under pure ammonia atmosphere after multiple prior absorption–desorption cycles. Squares represent trials at 170°C, triangles at 235°C, diamonds at 300°C, and circles at 365°C.

of the magnesium chloride absorbent.[10] If nanoporosity increases under our conditions, we would expect absorption rates to increase with absorbent use, the opposite of our observation. To explore this further, we measured the surface area by the BET method. As shown in Figure 4, these measurements involve plotting the equilibrium pressures of nitrogen measured in a fixed volume containing different amounts of solid. When these experiments are made with samples of silica–alumina zeolite calibration pellets we obtain an estimate of 200 m^2/g, consistent with measurements provided by the manufacturer (Micromeritics). However, when we make similar measurements with magnesium chloride, we get an area of 0.5 m^2/g. This is a strong argument against nanoporosity under high temperature conditions.

We also examined magnesium chloride crystals with a conventional optical microscope. We found that the structure size observed is on the order of microns, much smaller than the sieve-based structure size of 200 μm or larger. Used particles subjected to $\sim$ 50 cycles of absorption and desorption at 430°C and 5 atm pressure have an average structure size on the order of tens of microns, with occasional larger examples possessing diameters of several hundred microns. This means that there are different sizes involved: the constant larger structure found by sieving; and the smaller use-dependent structure, observed by microscopy. The larger size determined by sieving is time independent. It would affect any external, gas-phase mass transport limitation and pressure change caused by flow through the packed bed of these particles. The smaller structure size, observed by microscopy, increases with absorption and desorption of ammonia. We expect that this smaller structure size supplies surface area for absorption. The altered particle caused by using the absorbent, as well as the observation of crystal formation on the walls of the vessel, suggests that recrystallization occurs during the high-temperature absorption and desorption. If the smaller, micron sized structures get larger, the absorption should get slower. Thus, our measurements of decreased absorption rate, small BET surface area, and increased structure size are consistent.

We now turn to measures of absorption kinetics as a function of temperature and particle size. Typical data on used particles, shown in Figure 5, report changes in ammonia pressure as a function of time. Note that the uptake rate is very fast at small times, and that the total amount absorbed is reduced as the temperature rises. The fast uptake at small times is linear in the square root of time, as shown in Figure 6, consistent with the diffusion-based mechanism underlying Eq. 4. The reduced amount is consistent with the formation of different complexes: $Mg(NH_3)_6Cl_2$ at 70°C, $Mg(NH_3)_2Cl_2$ at 200°C, and $Mg(NH_3)Cl_2$ at 365°C.

The results in Figure 5 can be better understood if they are replotted as suggested by Eq. 5. In this equation, the logarithm of the measured pressure minus the equilibrium pressure is plotted vs. the square root of time. The same data now fall much more nearly on one straight line, as shown in Figure 6. Such variation with (time)$^{1/2}$ is strong evidence of a diffusion-based process. The data at 300 and 365°C overlap, suggesting that the permeability does not change with temperature over this range. This itself is surprising: whereas the diffusion in liquids is only a weak function of temperature, that in solids normally increases sharply. In addition, the data at 170 and 235°C also overlap, with a similar slope after about 4 s. Again, this is consistent with an unexpectedly temperature-independent permeability. We suspect that the minor differences observed in the initial pressure drop are due to changes in the complex state at different temperatures. We will detail how the diffusion coefficient can be estimated and discuss what chemistry this implies in the next section.

As previously stated, the above equations are only valid in the isothermal case. The expectation of temperature dependence of the diffusion coefficient would contribute nonlinear complexity to the analysis. Given the exothermic nature of the absorption, it is reasonable to expect that some method of temperature control is, therefore, necessary to maintain isothermal conditions. This is certainly the case in the first absorption–desorption cycle, where we observe an exotherm of $\sim$ 20°C. This may serve to explain in part the initially faster absorption rates in the fresh absorbent; we may be measuring the absorption rate at a temperature that is higher than reported. However, all subsequent cycles demonstrate exotherms less than 5°C on the time scale of the observed pressure drop. This minor exotherm is unlikely to significantly influence the diffusion coefficient and this behavior is an acceptable approximation of isothermal operation. All

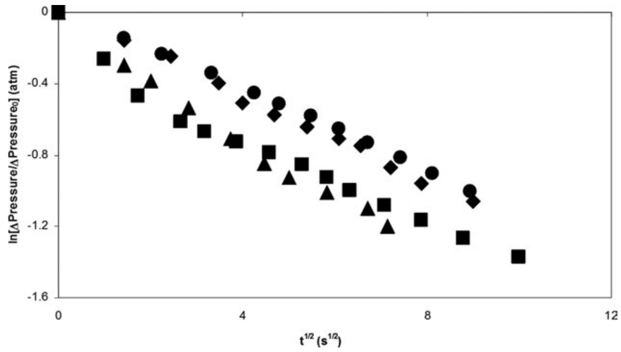

Figure 6. Ammonia absorption vs. (time)$^{1/2}$.

These data, for 5 g of unsupported $MgCl_2$ under pure ammonia atmosphere after multiple prior absorption–desorption cycles, are used with Eq. 5 to find the diffusivity at 175°C (squares), at 240°C (triangles), at 300°C (diamonds) and at 365°C (circles).

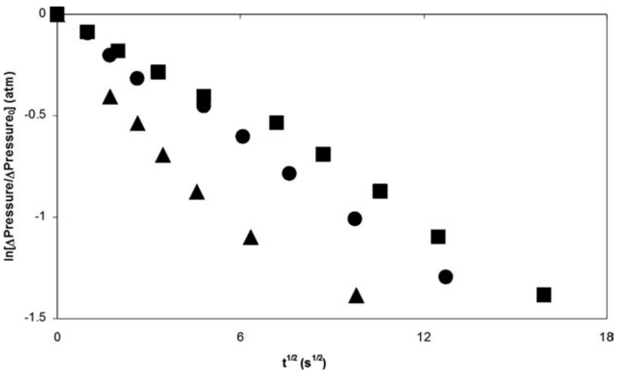

Figure 7. Ammonia uptake vs. nominal particle size at 430°C.

These data are plotted according to Eq. 5 for unsupported $MgCl_2$ samples having undergone multiple prior absorption–desorption cycles. The nominal particle size is that of the ground, sieved fresh absorbent initially loaded in the cell. Triangles are 100 μm particles, circles are 200 μm, and squares are 400 μm.

diffusion coefficient calculations present in this work, as well as all absorption rate data excepting Figure 3, were derived from experiments conducted on used magnesium chloride subjected to many cycles and which demonstrated minimal exotherms.

We also made some measurements of uptake rate vs. the nominal particle size, assigned by the size of the appropriate screen. As Figure 7 also shows, larger particles do absorb more slowly. These data raise the question of whether sieved particle size or microscopically observed structure size is most relevant. If the sieved structure size is key, then we expect in Eq. 5 that the total area A in that equation would be about

$$\frac{6m}{\rho d} \tag{6}$$

where m is the total absorbent mass, ρ is the density of the absorbent, and d is the size of the absorbent particles. Alternatively, if the microscopic structure size is key, then the total area should depend on the mass m but not on the sieved particle size d. The data in Figure 6 do show some variation with inverse size but less than an inverse relation. This implies a more complicated mechanism.

We had originally expected that any rapid uptake of ammonia would be due to the rapid adsorption of ammonia on the crystal surface, instead of absorption into the solid crystalline absorbent. To explore this expectation, we support magnesium chloride on Cab-o-sil ultraporous silica in an attempt to increase available surface area. The support could stabilize small, high capacity particles and restrain any particle growth and agglomeration that occurs during recrystallization. Supported magnesium chloride does demonstrate initial absorption rates two to three times faster than those of the supported material. This suggests that an increase in available surface area is achieved. However, after several cycles, the increase in absorption rate is lost and performance reverts to that of the unsupported magnesium chloride. The Cab-o-sil support does not seem to lend stability to the small particles or restrain particle growth during recrystallization at high-temperature cycling conditions. The magnesium chloride likely agglomerates during recrystallization in the same manner as the unsupported material.

Discussion

This research aims to simplify the process for producing ammonia. It seeks to increase conversion in the ammonia synthesis reaction by removing ammonia as it is formed. Although thin, ammonia selective membranes exist which could potentially do this, these membranes function only at temperatures well below the 360°C used in the reactor.[12–14] Moreover, because the reactor operates at pressures above 150 bar, the risk of using thin membranes will be serious. A better strategy is to remove the ammonia within the reactor without changes in pressure or temperature.

We can potentially remove the ammonia either by adsorption or by absorption. Adsorption involves capturing the ammonia on the surface of a nanoporous solid. However, even the surface of activated carbons or zeolites do not have the high capacity which we would like, as shown in Table 1. Moreover, we expect that the capacities shown in this table will be lost well before we reach the reactor temperatures. Adsorption does not seem sensible.

Thus, we turn to absorption, in which the ammonia actually diffuses into the solid. Ammonia absorption can have remarkably high capacities, even at high temperature, as shown in Table 1. However, diffusion coefficients in solids are often very small. For example, in ordinary liquids diffusion coefficients are typically 10^{-5} cm^2/s; but in crystalline solids, diffusion coefficients are characteristically 10^{-15}–10^{-40} cm^2/s. Thus, we worry that the high capacity of ammonia absorption is not useable because the rates of diffusion-controlled absorption are much too slow.

The results in Figure 6 show dramatically that absorption of ammonia in solid magnesium chloride is fast, with a half life of seconds. Thus, our expectation that absorption is too slow to improve ammonia synthesis is wrong. The time scale of ammonia synthesis in the Haber process is typically on the order of seconds,[1] meaning that the absorption will not significantly limit rate of ammonia production. Absorption has the potential to improve conversion and hence to simplify the ammonia synthesis.

The variation of ammonia pressure with the square root of time, a key to the data in Figure 6, is a strong signature of a diffusion-based process. Thus, we should be able to use Eq. 5 to estimate the diffusion coefficients involved. This is more difficult that it first appears, because this equation predicts that the slope of these data varies not only with the diffusion coefficient D but also with the partition coefficient H and the total crystal area A. The partition coefficients can be estimated from literature values of $MgCl_2$–NH_3 equilibria and complex densities derived from crystallographic theory.[8,15] The values at the temperatures where absorption has been studied in this work are given in Table 2. They are smaller as the temperature is larger, reflecting the reduced absorption.

The crystal area is more difficult to estimate, especially because the microscopy and the variation with cycles in

Table 2. Approximate Diffusion Coefficients of Ammonia in Anhydrous Magnesium Chloride

Temperature (°C)	Partition Coefficient (atm-cm^3/mol)	Diffusion Coefficient (cm^2/s)
170	2.2×10^{-2}	1.0×10^{-13}
235	1.5×10^{-3}	2.9×10^{-11}
300	7.5×10^{-4}	5.0×10^{-11}
365	6.1×10^{-4}	5.2×10^{-11}

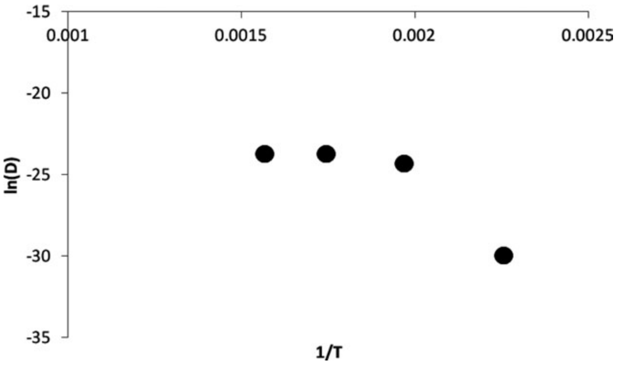

Figure 8. Arrhenius plot of temperature-dependent diffusion.

Plot of reciprocal temperature (where *T* is in Kelvin) vs. the logarithm of the calculated diffusion coefficient (where *D* is in cm^2/s). The slope and intercept provide empirical values for ΔH and D_0, respectively.

Figure 3 show that the crystals do not have constant size. However, the BET data in Figure 4 suggest a size given by

$$0.5 \cdot 10^4 \frac{\text{cm}^2}{\text{g}} \left(\frac{2.32\text{g}}{\text{cm}^3}\right) = \frac{6}{d}$$
$$d = 5\,\mu\text{m}$$

This implies that 5-μm crystals are slightly agglomerated, with most of their area of 0.5 m^2/g still available for absorption.

Using these values of H and A, we estimate the values of the diffusion coefficient D in Table 2. These values are about a million times less than those in a liquid and 10,000 times less than values in a polymer solution, but billions of times greater than those in many crystalline solids. Although we believe that they are reliable, we are unsure why they are so fast. Still, the diffusion coefficients do behave as expected. The values do exhibit the increase with increasing temperature that we would expect for diffusion in a solid. The small temperature dependence of the absorption rates in Figure 6 turns out to be a result of a partition coefficient which decreases with temperature, balanced by a diffusion coefficient that increases with temperature. The logarithm of the estimated diffusion coefficient has been plotted against the reciprocal of the absolute temperature to yield the Arrhenius plot in Figure 8. The ΔH implied by the data is $\sim$ 12 kJ/mol, much less than the $>$100 kJ/mol typical of most solids.[9] The outlier at 170°C may be due to the altered stoichiometry and crystal structure present at that temperature.

These results suggest two very different potential applications. The first application, which has minimum risk, simplifies the separation of the partially reacted gases exiting the Haber process reactor. At present, this mixture of hydrogen, nitrogen, and ammonia is cooled, either to permit ammonia condensation or to allow washing the gases with water to produce aqueous ammonia solutions. In either case, the uncondensed gases are then reheated for recycle into the Haber process reactor.

The alternative is to separate the gas mixture using pressure swing absorption (PSA) based on the magnesium chloride. To our knowledge, there is no process data on such a system. However, we do note that PSA is already used earlier in the existing ammonia process, to remove carbon dioxide from the hydrogen–nitrogen mixture before this mixture is fed to the Haber process reactors.

The second potential application, which has major risk, involves a simplified ammonia synthesis suitable not for a large, centralized plant but for a small-scale dispersed manufacture. In such a plant, we propose obtaining nitrogen from noncryogenic, hollow fiber membrane separation of air and hydrogen from the electrolysis of water. Both membrane separation and electrolysis are well-established technologies. Membrane separation is more economical than cryogenic distillation at small scales like those sought here. Similarly, hydrogen manufacture by electrolysis has been practiced since 1800. Although it is more expensive compared with hydrogen made from cheap hydrocarbon fuels, electrolysis is powered by sustainable sources of electricity, especially wind power.

We could mix Haber process catalyst and magnesium chloride. Now, the process is fed with hydrogen and nitrogen until the magnesium chloride is saturated with ammonia. The feed is then stopped and the pressure released to recover the ammonia. This fed-batch reactor, very different than the existing process, would be like a large diesel engine turning over perhaps 0.3 rpm. Its lower capital investment and its modest size could make it an attractive route to dispersed ammonia manufacture, either at an agricultural co-op or on a large individual farm.

Acknowledgments

This work was principally supported by the Initiative for Renewable Energy and the Environment (IREE) at the University of Minnesota. Other support came from the Dow Chemical Company.

Literature Cited

1. Twigg MV. *Catalyst Handbook*. London: Wolfe, 1989.
2. Christensen CH, Sorensen RZ, Johannessen T, Quaade UJ, Honkala K, Elmoe TD, Kohler R, Norskov JK. Metal ammine complexes for hydrogen storage. *J Mater Chem.* 2005;15:4106–4108.
3. Katada N, Igi H, Kim J, Niwa M. Determination of the acidic properties of zeolite by theoretical analysis of temperature-programmed desorption of ammonia based on adsorption equilibrium. *J Phys Chem B*. 1997;101:5969–5977.
4. Liu CY, Aika K. Ammonia absorption on alkaline earth halides as ammonia separation and storage procedure. *Bull Chem Soc Jpn.* 2004;77:123–131.
5. Liu CY, Aika K. Ammonia absorption into alkaline earth metal halide mixtures as an ammonia storage material. *Ind Eng Chem Res.* 2004;43:7484–7491.
6. Liu CY, Aika K. Modification of active carbon and zeolite as ammonia separation materials for a new de-NO$_x$ process with ammonia on-site synthesis. *Res Chem Intermed.* 2002;28:409–417.
7. Long X, Cheng H, Lin Z, Xiao W, Li W, Yuan W. Adsorption of ammonia on activated carbons from aqueous solutions. *Environ Prog.* 2008;27:225–233.
8. Elmoe TD, Sorensen RZ, Quaade U, Christensen CH, Norskov JK, Johannessen T. A high-density ammonia storage/delivery system based on $Mg(NH_3)_6Cl_2$ for SCR-DeNO$_x$ in vehicles. *Chem Eng Sci.* 2006;61:2618–2625.
9. Cussler EL. *Diffusion: Mass Transfer in Fluid Systems*. Cambridge: Cambridge University Press, 2009.
10. Hummelshoj JS, Sorensen RZ, Kustova MY, Johannessen T, Norskov JK, Christensen CH. Generation of nanopores during desorption of NH_3 from $Mg(NH_3)_6Cl_2$. *J Am Chem Soc.* 2006;128:16–17.
11. David ME, Davis RJ. *Fundamentals of Chemical Reaction Engineering*. Boston: McGraw-Hill, 2003.
12. Bhown A, Cussler EL. Mechanism for ammonia transport through poly(vinylammoniumthiocyanate) membranes. *J Am Chem Soc.* 1991;113:742–749.
13. He Y, Cussler EL. Ammonia permeabilities of perfluorosulfonic membranes in various ionic forms. *J Membr Sci.* 1992;68:43–52.
14. Phillip WA, Martono E, Chen L, Hillmyer MA, Cussler EL. Seeking an ammonia selective membrane based on nanostructured sulfonated block copolymers. *J Membr Sci.* 2009;337:39–46.
15. Tekin A, Hummelshoj JS, Jacobsen HS, Sveinbjornsson D, Blanchard D, Norskov JK, Vegge T. Ammonia dynamics in magnesium ammine from DFT and neutron scattering. *Energy Environ Sci.* 2010;3:448–456.

Appendix

Sample diffusion coefficient calculation

The diffusion coefficient of ammonia in magnesium chloride inferred from the experimental data by Eq. 5:

$$D = \left(\frac{-s}{H(A/V)RT}\sqrt{\frac{\pi}{2}}\right)^2$$

where A is the specific surface area, V is the cell volume, H is a partition coefficient, R is the gas constant, T is the temperature, and s is the slope of the experimental data. The magnesium chloride specific surface area is determined by BET:

$$A = 4800\frac{\mathrm{cm}^2}{\mathrm{g}}$$

The volume of the absorption cell is:

$$V = 55.0\mathrm{cm}^3$$

The slope is determined from the experimental absorption data when the logarithm of the dimensionless pressure change is plotted against the square root of time:

$$s = \frac{d\left(\ln\left(\frac{\Delta p}{\Delta p_0}\right)\right)}{d(t^{-1/2})} = -0.126\,\mathrm{s}^{-1/2}$$

The experimental temperature is:

$$T = 443\mathrm{K}$$

The gas constant is:

$$R = 82.06\frac{\mathrm{cm}^3\mathrm{atm}}{\mathrm{molK}}$$

The experimental equilibrium pressure is determined from overnight trial and is used in the calculation of the partition coefficient and in the pressure change data to provide the slope of the experimental data:

$$p_{\mathrm{NH_3,eq}} = 0.07\mathrm{atm}$$

The density of $MgCl_2(NH_3)_2$ is determined using literature values of crystallographic parameters. The second complex is that present at 443 K:

$$\rho = 1.84\frac{\mathrm{g}}{\mathrm{cm}^3}$$

The mass of anhydrous $MgCl_2$ initially loaded into the absorption cell is:

$$m = 5.0\ \mathrm{g}$$

The ratio of the molecular weights of anhydrous magnesium chloride and the second complex is:

$$r = \frac{M_\mathrm{w}\mathrm{MgCl_2(NH_3)_2}}{M_\mathrm{w}\mathrm{MgCl_2}} = 1.36$$

The experimental pressure difference from overnight trial to be used in the experimental slope determination is:

$$p_0 = 3.79\ \mathrm{atm}$$

The experimental equilibrium concentration of ammonia in magnesium chloride is determined by measuring the pressure change overnight and applying an ideal gas law to determine the number of moles of ammonia absorbed. The ratio of molecular weights, the initial mass, and the complex density are used to calculate the volume of the complex present:

$$C_{\mathrm{NH_3,eq}} = \frac{V\Delta p}{RT}\frac{1}{(rm/\rho)} = \frac{55.0\times 3.79\times 1.84}{443\times 82.06\times 5.0\times 1.36} = 1.57\times 10^{-3}\frac{\mathrm{g}}{\mathrm{cm}^3}$$

The partition coefficient is simply the ratio between the experimentally determined equilibrium concentration of ammonia in the complex and the equilibrium gas pressure of ammonia in the cell:

$$H = \frac{C_{\mathrm{NH_3,eq}}}{p_{\mathrm{NH_3,eq}}} = \frac{1.57\times 10^{-3}}{0.07} = 2.24\times 10^{-2}\ \frac{\mathrm{g/cm}^3}{\mathrm{atm}}$$

The diffusion coefficient is easily estimated from Eq. 5, as described previously:

$$D = \left(\frac{-s}{H(A/V)RT}\sqrt{\frac{\pi}{2}}\right)^2 = \left(\frac{1.26\times 10^{-1}\times\sqrt{\pi/2}}{2.24\times 10^{-2}\times(4800/55.0)\times 82.1\times 443}\right)^2 = 2.0\times 10^{-13}\frac{\mathrm{cm}^2}{\mathrm{s}}$$

Manuscript received Aug. 7, 2011, and revision received Dec. 15, 2011.